Converting a Maltose Receptor into a Nascent Binuclear Copper Oxygenase by Computational Design†

David E. Benson,‡ Alice E. Haddy,§ and Homme W. Hellinga*,||

Department of Chemistry, 221 Petty Building, University of North Carolina-Greensboro, Greensboro, North Carolina 27402, and Department of Biochemistry, Box 3711, Duke University Medical Center, Durham, North Carolina 27710

Received June 27, 2001

ABSTRACT: Computational protein design methods were used to identify mutations that are predicted to introduce a binuclear copper center coordinated by six histidines, replacing the maltose-binding site in *Escherichia coli* maltose-binding protein (MBP) with an oxygen-binding site. A small family of five candidate designs consisting of 9 to 10 mutations each was constructed by oligonucleotide-directed mutagenesis. These mutant proteins were expressed and purified, and their stability, copper- and cobalt-binding properties, and interactions of the resulting metalloprotein complexes with azide, hydrogen peroxide, and dioxygen were characterized. We identified one 10-fold mutant, MBP.Hc.E, that can form Cu^{II}_2 and Co^{II}_2 complexes that interact with H_2O_2 and O_2. The Co^{II}_2 protein reacts with H_2O_2 to form a complex that is spectroscopically similar to a synthetic model that structurally mimics the oxy-hemocyanin core, whereas the Cu^{II}_2 protein reacted with O_2 or H_2O_2 does not. We postulate that the equilibrium between the open and closed conformations of MBP allows species with variable Cu−Cu distances to form, and that such species can bind ligands in geometries that are not observed in natural type III centers. Introduction of one additional mutation in the hinge region of MBP, I329F, known to favor formation of the closed state, results in a binuclear copper center that when reacted with low concentrations of H_2O_2 mimics the spectroscopic signature of oxy-hemocyanin.

Rational protein design is emerging as a technique for identifying factors that contribute to the control of metal center formation and reactivity (*1*−*4*). In particular, rational design is a powerful approach for uncovering competing states that do not form in naturally evolved systems (*5*, *6*). In this way, it has been shown that mechanisms for control of reactivity involve a mixture of stabilization of desired states and destabilization of competing states (*7*−*9*). Here we use computational design techniques (*1*, *2*, *6*) to investigate the factors that are necessary to convert the *Escherichia coli* maltose-binding protein (MBP) into a oxygen-binding protein, by introducing a binuclear copper ("type III") center in place of wild-type maltose-binding residues. Such centers can either reversibly bind oxygen or activate oxygen, and are found in oxygen carrier proteins such as hemocyanin, or enzymes such as tyrosinase or catechol oxidase (*10*). Proteins containing these centers are involved in a diverse set of biochemical processes, ranging from oxygen transport, biodegradation, melanin production, and potentially hydrocarbon metabolism (*10*).

MBP is a member of a superfamily of bacterial chemoreceptors (*11*). It consists of a single polypeptide chain that folds into two globular domains connected by a hinge region, with the maltose-binding pocket being located within the interdomain interface (*12*). MBP exists in two conformations that are in equilibrium: a ligand-free open form and a liganded closed form (Figure 1A). The periplasmic binding protein superfamily binds a wide diversity of ligands, ranging from carbohydrates, amino acids, neurotransmitters, and oligopeptides to anions and cations (*11*). Thus far, no oxygen-binding member of the family has been identified. The remarkable diversity in molecular recognition exhibited within this superfamily is likely to be the consequence of the ligand-binding sites being located at the interface between two domains (*13*). In this arrangement, residues forming the binding site are placed at the surface of the domains, yet in forming a complex the ligand is situated in an environment that resembles the interior of a protein. The advantages of the structural plasticity associated with making mutations on protein surfaces are therefore combined with the enhanced control of chemical reactivity that can be achieved within a site that is shielded from solvent. MBP is therefore an excellent candidate for introducing potentially highly reactive

† This work was supported by grants from the National Institutes of Health (R01GM49871, H.W.H.) and a Fellowship (GM19459-01A1, D.E.B.).

* To whom correspondence should be addressed, Dr. Homme W. Hellinga, Department of Biochemistry, Box 3711, Duke University Medical Center, Durham, NC 27710; e-mail, hwh@biochem.duke.edu.

§ University of North Carolina-Greensboro.

|| Duke University Medical Center.

‡ Present address: Department of Chemistry, Wayne State University, Detroit, MI 48202

[1] Abbreviations: MBP, *E. coli* maltose binding protein; MBP.Hc.-(A−E), 9−10-fold mutants of MBP that are designed to assemble a binuclear copper oxygen center similar to oxy-hemocyanin; type III Cu center, magnetically coupled binuclear copper center; oxy-Hc, the oxygenated form of hemocyanin; CD, circular dichroism; EPR, electron paramagnetic resonance; Cu^{II}_1·MBP.Hc.E, MBP.Hc.E with one equivalent of Cu^{II} bound; Cu^{II}_2·MBP.Hc.E, MBP.Hc.E with two equivalents of Cu^{II} bound; Cu^{II}_2·MBP.Hc.E·H_2O_2, the H_2O_2 adduct of Cu^{II}_2·MBP.Hc.E; Cu^{I}_2·MBP.Hc. E·O_2, the O_2 adduct of Cu^{I}_2·MBP.Hc.E; Co^{II}_2·MBP.Hc.E, MBP.Hc.E with two equivalents of Co^{II} bound; Co^{II}_2·MBP.Hc.E·H_2O_2, the H_2O_2 adduct of Co^{II}_2·MBP.Hc.E.

10.1021/bi011359i CCC: $22.00
Published on Web 02/08/2002

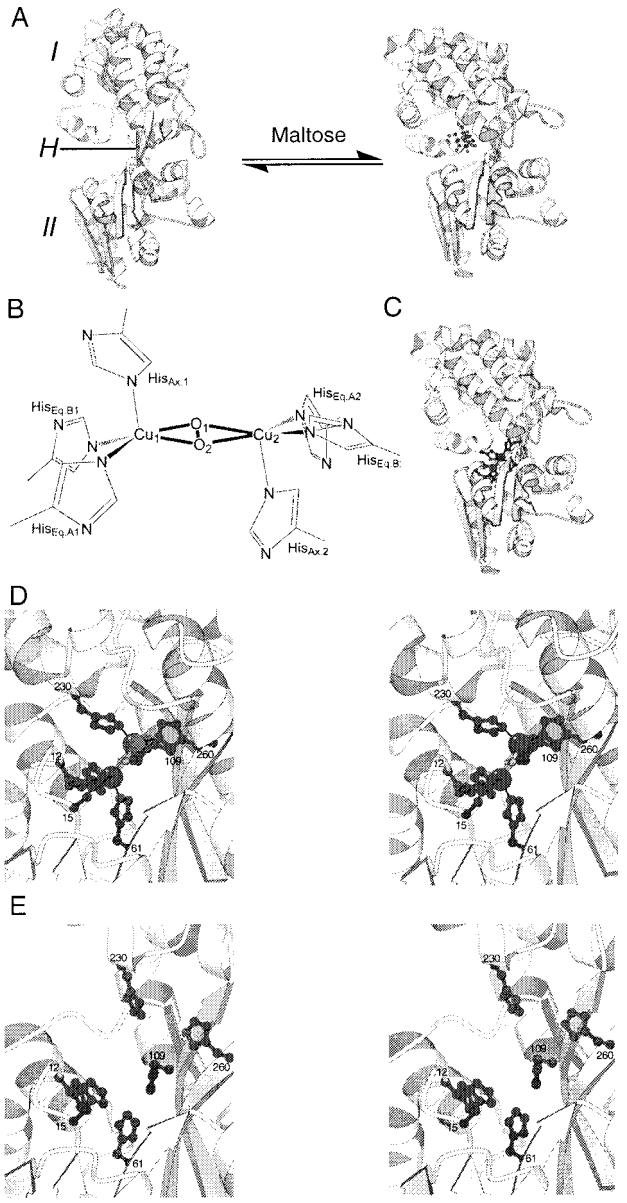

FIGURE 1: Design of a binuclear copper oxygen active site in maltose-binding protein (MBP). (A) Binding of maltose induces a conformational change from an open conformation (*56*) (left; pdb accession number, 1OMP) to a closed conformation (*12*) (right; pdb accession number, 1ANF). (B) Structure of the binuclear copper oxygen center used for model construction. (C) Location of the copper oxygen active site in MBP.Hc.E (closed conformation), as predicted by the *Dezymer* program. (D) Detailed stereoviews of the predicted binuclear copper binding site in MBP.Hc.E (numbers indicate the residue positions of the six histidines forming the primary coordination sphere) in the closed state, and (E) in the open state. Molecular graphics were prepared using Molscript (*57*).

binuclear copper oxygen centers that are notorious for exhibiting side reactions, due to the large number of energetically degenerate, but chemically diverse, reactions available to the aqueous ion under physiological conditions (*14*).

Rational design of metalloproteins that bind and activate small ligands, such as O_2, N_2, and H_2, is a formidable challenge in protein science and bioinorganic chemistry (*1*, *3*, *7*, *15*−*17*). Recently, non-heme iron centers have been introduced into *E. coli* thioredoxin (*7*) and a four-helix bundle peptide assembly (*18*), which display nascent metalloxygenase properties. Both of these designed non-heme iron proteins [$FeHis_3$ (*7*) or $Fe_2(\mu\text{-O})(\mu\text{-Asp})_2His_4$ (*18*)] represent a wide array of substrate oxidations and physiological responses (*19*). Thus far, the design of binuclear copper centers has not been explored. There are a number of factors that make the design of binuclear copper centers more tractable than binuclear iron centers: the spectroscopic addressability (UV−visible absorbance) of Cu_2-O_2 centers (*10*, *20*), utilization of lower oxidation states by copper-mediated oxidations (*20*, *21*), and formation of copper centers by less polar ligands (*22*).

EXPERIMENTAL PROCEDURES

Buffers were made metal free by dithiazone (recrystalized)/chloroform extractions (*23*). All other chemicals were used without further purification. The concentration of H_2O_2 stock solutions was quantified by direct titration with potassium permanganate.

Molecular Modeling. Mutations in MBP necessary to introduce a binuclear copper sites were predicted using the *Dezymer* algorithm (*24*) and are based on the structure of MBP complexed with maltose (*12*) (1ANF pdb accession ID).

Protein Mutagenesis, Expression, and Purification. Mutations in maltose binding protein were constructed by oligonucleotide-directed mutagenesis and verified by DNA sequencing. Mutant proteins (MBP.Hc) were produced by overexpression in BL-21(DE3), fermented in Terrific Broth (*25*) by growth at 37 °C, induced with 1 mM IPTG when OD_{600} reached 0.5, followed by additional growth at 20 °C for 12 to 16 h. A cleared lysate (*26*) of these cells was dialyzed (30 000 MW cutoff, four exchanges of 30 min each) against 10 mM Tris (pH 8.0) and loaded on a Q-sepharose (HiTrap 16/10 Q XL, Pharmacia). The Q-sepharose column was washed with four column volumes of buffer, and eluted with a linear gradient from 0 to 400 mM NaCl (10 column volumes). Fractions containing MBP were identified by SDS−PAGE, incubated with 1 mM *o*-phenanthroline and 5 mM EDTA for 1 h, concentrated by ultrafiltration (YM-30, Amicon), and further purified by gel filtration (Hi Trap 26/60 Sephacryl S-100, Pharmacia), preequilibrated with 20 mM Tris (pH 7.5) 100 mM NaCl (TS), to 95−99% purity. Protein concentrations were determined either by the Edelhoch method (*27*) (apo-protein) or by the Bradford method (*28*) (metalloprotein), using apo-protein as an internal standard. All subsequent experiments were performed in TS buffer.

Circular Dichroism (CD). Wavelength scans or temperature denaturation curves (using 222 nm to monitor protein folding) were measured using 3 mL, 1 μM MBP.Hc in a sealed 1-cm path length quartz cuvette (Helma) with a CD spectrophotometer (Aviv model 202). Thermal denaturations were fit to standard equations for calculating T_M (*29*).

Cu^{II} Addition. A solution of 10 mM $CuSO_4$ was titrated into 100 μM MBP.Hc, using absorbance at 325 nm to monitor complex formation. Absorbance changes were fit to standard binding isotherms to calculate dissociation constants (*4*). Cu^{II} in content in purified protein fractions was determined spectrophotometrically using bathocuprein (*30*).

EPR Spectroscopy. Spectra of frozen samples (liquid N_2) of 100 μM MBP.Hc in quartz tubes (Wilmad) were obtained with a Bruker EMX 6/1 spectrometer (ER 4116 DM dual

Table 1: Designed MBP.Hc Sites

site	mutations[a] vertex A	vertex B	steric[b]	CD T_m (°C)	$Cu^{II}K_d$ (μM)	$N_3^-K_d$ (mM)	$H_2O_2K_d$ (μM)
A	$W^{I}230H_\epsilon$, $K^{II}15H_\delta$, $L^{II}299H_\delta$	$N^{II}12H_\epsilon$, $F^{II}61H_\epsilon$, $A^{II}63H_\epsilon$	$E^{H}111A$, $L^{H}262A$, $I^{II}11A$, $D^{II}14N$	none[c]	>250		
B	$W^{I}230H_\epsilon$, $E^{H}111H_\epsilon$, $L^{II}299H_\delta$	$N^{II}12H_\epsilon$, $K^{II}15H_\delta$, $F^{II}61H_\epsilon$	$L^{H}262A$, $I^{II}11A$, $D^{II}14N$	45	>250		
C	$W^{I}230H_\epsilon$, $N^{II}12H_\epsilon$, $A^{II}63H_\epsilon$	$A^{H}109H_\epsilon$, $K^{II}15H_\delta$, $F^{II}61H_\epsilon$	$E^{H}111A$, $L^{H}262A$, $I^{II}11A$, $D^{II}14N$	55	>250		
D	$W^{I}230H_\epsilon$, $K^{II}15H_\delta$, $L^{II}299H_\delta$	$L^{H}262H_\delta$, $N^{II}12H_\epsilon$, $A^{II}63H_\epsilon$	$E^{H}111A$, $I^{II}11A$, $D^{II}14N$	51	60	100	>100[d]
E	$W^{I}230H_\epsilon$, $A^{H}109H_\epsilon$, $G^{H}260H_\epsilon$	$N^{II}12H_\epsilon$, $K^{II}15H_\delta$, $F^{II}61H_\epsilon$	$E^{H}111A$, $L^{H}262A$, $I^{II}11A$, $D^{II}14N$	50	20	50	15

[a] Superscripts denote location of the residue within one of the two domains (I,II) or hinge region (H). Histidine mutant subscripts denote the nitrogen atom coordinating to a copper atom. [b] Mutations predicted to alleviate unfavorable steric contacts. [c] CD spectrum at 25 °C displayed a minimum at 222 nm of moderate intensity. This protein does not exhibit two-state thermal denaturation. [d] Lower estimate, due to complications associated with sample precipitation.

mode cavity; frequency, 9.648 GHz; modulation, 0.63 mW) at 10 K (Oxford ESR 900 cryostat).

Azide and Hydrogen Peroxide to Cu^{II}-Containing Samples. H_2O_2 or NaN_3 were titrated into a 1-mL sample containing MBP.Hc (100 μM) and $CuSO_4$ (200 μM); absorbance changes at 310 or 360 nm, respectively, were fit to binding isotherms (*4*). The H_2O_2-saturated sample was subsequently purified on a gel filtration column (PD-10, Pharmacia).

Addition of Oxygen to Reduced Cu^{II}-Containing Samples. A sample of 100 μM MBP.Hc was purged with nitrogen, $CuSO_4$ was added to a final concentration of 200 μM, reduced with $Na_2S_2O_4$ which was added until a slight excess ($\sim$ 25 μM) of unreacted $Na_2S_2O_4$ was observed at 312 nm (ϵ = 6220 M^{-1} cm^{-1}). A stream of pure oxygen was then passed through the cuvette for 5 min, and the resulting UV−visible spectrum of the sample recorded. The resulting complex was subsequently purified on a gel filtration column (PD-10, Pharmacia).

Addition of Oxygen and Hydrogen Peroxide to Co^{II}-Containing Samples. An anerobic solution of $CoCl_2$ was added (200 μM final concentration) to a degassed sample of MBP.Hc (100 μM). Potential formation of complexes formed upon addition of dioxygen (100% O_2, 2 h) or H_2O_2 (addition 1:10 dilution of 30% stock) was monitored spectrophotometrically. The H_2O_2-saturated solution of Co^{II}_2·MBP.Hc was purified (PD-10, Pharmacia) and reduced with dithionite, or irradiated with 5 mW at 514.5 nm (Ar^+ laser, Spectra-Physics series 2000) or a 450 W Xe arc lamp (1 nm bandwidth, Aviv model 202), to investigate susceptibility to photolysis.

RESULTS

Design. Mutations predicted to introduce a binuclear copper center into the closed structure of MBP were calculated using the *Dezymer* algorithm (*24*). This center consists of a binuclear Cu^{II}_2 core with O_2^{2-} complexed in a bridging $\mu-\eta_2:\eta_2$ coordination geometry, with each Cu vertex coordinated by a His_3 tripod in an approximately square pyramidal geometry (Figure 1). The geometry of the Cu_2O_2 core was taken from the oxy-hemocyanin (oxy-Hc) structure (*31*) (pdb accession number, 1NOL). The structure of the closed conformation (with the maltose coordinates removed) was used in the calculations (*12*) (pdb accession number, 1ANF). The predictions were generated using purely geometrical criteria to describe the coordination sphere of the binuclear center, and a hard-sphere model to evaluate steric compatibility with the protein backbone in the absence of other side-chain residues. The bonding between each histidine and its cognate Cu vertex was constrained to a σ-bond geometry, allowing the metal to coordinate through either N_ϵ or N_δ, with 2.1 Å (equatorial) or 2.4 Å (axial) bond lengths, and constraining the metal to lie within the imidazole plane with bond angles corresponding to sp^2 hybridization for the coordinating nitrogen. The bond angles for each Cu vertex were constrained to square pyramidal geometry. The axial histidines in each tripod were allowed to be either trans (oxy-Hc) or cis [several model complexes (*32*)] relative to each other. Placement of these centers was limited to the interdomain interface of MBP, in the vicinity of the wild-type maltose-binding site (Figure 1), with the additional constraint that the six histidines are distributed between both domains, such the binuclear copper oxygen center can form only in the closed state (*33*). After positioning of the primary coordination sphere, carried out in the absence of other side-chains, additional mutations required to alleviate unfavorable steric contacts between the surrounding protein matrix and the designed center, were identified by inspection.

Fifty candidate sites were generated in the initial calculations. These were rank ordered based on a score that captures how well a site geometry approximates an idealized center, and how many additional mutations are necessary to remove unfavorable steric contacts between a site and the surrounding, wild-type, protein matrix. The five sites that ranked highest by these criteria (MBP.Hc.A−E)[2] were constructed by mutagenesis (Table 1) to construct a small family of designs (*7*, *9*), from which one design was selected for detailed characterization (Figure 1). Each of the designs required several additional mutations in the surrounding protein matrix to alleviate unfavorable steric contacts (Table 1).

Protein Stability. All five designs were expressed and purified, and their CD spectra determined. The stability of the mutants in the absence of metal was determined by thermal denaturation, and compared to wild-type MBP (Table 1). With the exception of MBP.Hc.A, the CD spectra were similar in shape and molar ellipticity as compared to wild-type MBP, and showed two-state unfolding transitions with midpoint temperatures of 45−55 °C (as compared to 68 °C observed for wild-type apo-MBP). MBP.Hc.A has significantly diminished molar ellipticity at 222 nm, and does not exhibit cooperative denaturation; it was therefore eliminated from further consideration.

Maltose Binding. None of the designs bound maltose (K_d > 5 mM), as determined by monitoring the change in tryptophan fluorescence upon addition of maltose (data not shown).

[2] Naming does not imply a rank order.

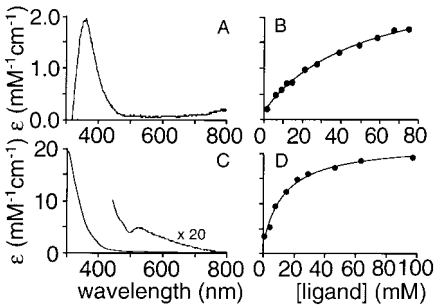

FIGURE 2: Addition of N_3^- and H_2O_2 to Cu^{II}_2·MBP.Hc. (A) Difference spectrum of a Cu^{II}_2·MBP.Hc.E sample with 80 mM NaN_3, relative to the apo-protein. (B) Binding isotherm of the NaN_3 titration, monitored by absorbance changes at 360 nm (K_D = 50 mM). (C) Difference spectrum of Cu^{II}_2·MBP.Hc.E with 100 mM H_2O_2, relative to the apo-protein. (D) Binding isotherm of the H_2O_2 titration, monitored by absorbance changes at 310 nm (K_D = 15 mM).

Cu^{II} Binding. Binding of $CuSO_4$ was monitored by identifying changes in absorbance relative to the apo-protein and to Cu^{II} in protein-free, buffered solution. By this criterion, MBP.Hc.B and MBP.Hc.C did not bind Cu^{II} (K_d > 250 μM) and therefore were eliminated from further consideration. The absorbance observed at 325 nm was used to determine the Cu^{II} affinity for MBP.Hc.D and MBP.Hc.E, by fitting to binding isotherms of either one or two equivalents of Cu^{II} (100 μM protein). In both cases, binding of two Cu^{II} equivalents were found to best fit the data, with affinities of 50 and 20 μM for MBP.Hc.D and MBP.Hc.E, respectively.

Azide Binding. Binding of small ligands was probed by the addition of azide to the Cu^{II}_2 sample (100 μM protein, 200 μM $CuSO_4$). Addition of azide resulted in spectral changes (Figure 2A) that allowed a dissociation constant to be determined by fitting the absorbance at 360 nm to a binding isotherm (Figure 2B), which were found to be 100 and 50 mM for MBP.Hc.D and MBP.Hc.E, respectively [as compared to 1−50 mM observed for various hemocyanins (*34*)].

Addition of H_2O_2. Titration of H_2O_2 to the Cu^{II}_2 sample of MBP.Hc.E (100 μM protein, 200 μM $CuSO_4$) resulted in a species (Cu^{II}_2·MBP.Hc.E·H_2O_2) with an extinction coefficient[3] at 310 nm of 20 000 M^{-1} cm^{-1} (Figure 2C) and fit to a binding isotherm (Figure 2D) with a dissociation constant of 15 mM. Addition of up to 300 μM H_2O_2 to a mononuclear Cu^{II} complex designed into the same region of MBP (*33*) did not result in significant absorbances in this region (above 300 μM H_2O_2 this control protein precipitates). Separation of protein in this sample from free Cu^{II} and H_2O_2 on a gel filtration column retains the initially observed spectral properties and maintains two equivalents of Cu^{II} per protein, suggesting that a stable complex is formed (Cu^{II}_2·MBP.Hc.E·H_2O_2).

Spectral changes similar to those observed for MBP.Hc.E were seen upon addition of H_2O_2 to MBP.Hc.D, but analysis was hampered by protein precipitation. MBP.Hc.D was therefore eliminated from further consideration.

EPR Spectroscopy. Spectra were recorded for MBP.Hc.E in the presence of one (Cu^{II}_1·MBP.Hc.E) and two equivalents of Cu^{II} (Cu^{II}_2·MBP.Hc.E), and for the H_2O_2-treated Cu^{II}_2 sample (Cu^{II}_2·MBP.Hc.E·H_2O_2) (Figure 3). The integrated intensity of the Cu^{II}_2·MBP.Hc.E sample was twice that of the Cu^{II}_1·MBP.Hc.E; these integrated intensities were similar to those observed for equivalent concentrations of Cu^{II} in protein-free buffer. Addition of H_2O_2 to the Cu^{II}_2·MBP.Hc.E sample formed the previously observed Cu^{II}_2·MBP.Hc.E·H_2O_2 species, for which no detectable EPR signal was observed between 500 and 4500 G at either 4 or 10 K. Addition of H_2O_2 to protein-free Cu^{II} in buffer retained the low-spin resonance observed in the absence of H_2O_2.

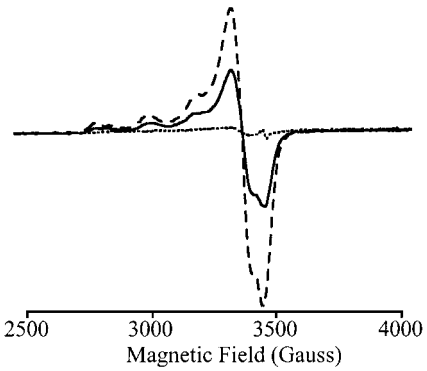

FIGURE 3: EPR spectra of Cu^{II}·MBP.Hc.E samples. Solid line: one equivalent of Cu^{II} (Cu^{II}_1·MBP.Hc.E); dashed line: two equivalents of Cu^{II} (Cu^{II}_2·MBP.Hc.E); dotted line: the spectrum observed after the addition of 50 mM H_2O_2 to Cu^{II}_2·MBP.Hc.E.

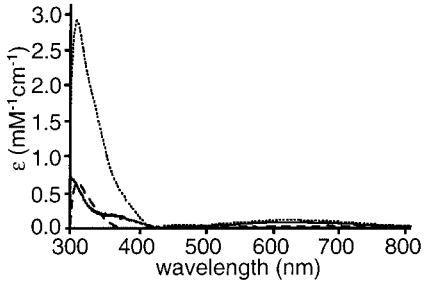

FIGURE 4: Oxygenation of Cu^{I}_2·MBP.Hc.E. An anaerobic solution of Cu^{II}_2·MBP.Hc.E (solid line) was reduced to Cu^{I}_2·MBP.Hc.E (dashed line) by addition of a slight excess of dithionite, and then exposed to a stream of O_2 for five minutes to form Cu^{I}_2·MBP.Hc.E·O_2 (dotted line).

Oxygenation. A solution of MBP.Hc.E with two equivalents of Cu^{II} was reduced with dithionite, and exposed to a stream of 100% O_2. The resulting solution exhibits similar electronic absorbances as observed for Cu^{II}_2·MBP.Hc.E·H_2O_2 (Figure 4), albeit with reduced intensity[3] ($\epsilon_{310} \sim 3000$ M^{-1} cm^{-1}),[4] and a *d-d* transition at 620 nm ($\epsilon_{620} \sim 80$ M^{-1} cm^{-1}). The observed spectral properties change upon gel filtration, with a retention of the spectrum, but with a 2-fold reduction in intensity in the 300−400 nm region, and loss of 1.5 ± 0.25 equivalents of Cu^{II}. Purging with N_2 following oxygenation and prior to gel filtration did not change the absorbance. Addition of dithionite did result in loss of the observed spectrum, however.

Oxygenation and Peroxidation of Co^{II} Complexes. Addition of two equivalents of $CoCl_2$ to MBP.Hc.E yielded a species with a broad absorbance (Figure 5) ranging from 400 to 550 nm ($\epsilon_{550} \sim 50$ M^{-1} cm^{-1}). Exposure to a stream of

[3] Extinction coefficients are reported using the known apo-protein concentration to normalize the maximum observed absorbance.

[4] It should be noted, however, that the solubility limit of oxygenated buffers is ~1.2 mM at 25 °C (*36*) and that it is therefore not known whether the observed complex is saturated.

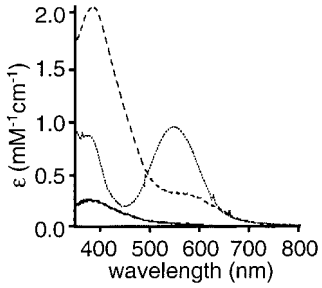

FIGURE 5: Addition of H_2O_2 to Co^{II}_2·MBP.Hc.E. Three difference spectra are shown relative to the apo-protein. Solid line: Co^{II}_2·MBP.Hc.E; dashed line: Co^{II}_2·MBP.Hc.E with five equivalents of H_2O_2 (Co^{II}_2·MBP.Hc.E·H_2O_2 brown species); dotted line: the Co^{II}_2·MBP.Hc.E·H_2O_2 species after 30-min exposure to visible light (Co^{II}_2·MBP.Hc.E·H_2O_2 pink species).

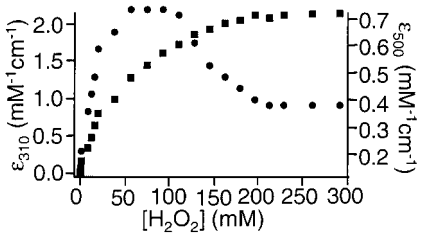

FIGURE 6: Titration of Cu^{II}_2·MBP.Hc.E1 (I329F) with H_2O_2. Squares (left axis): change in absorbance monitored at 310 nm; circles (right axis): change of absorbance monitored at 500 nm. The biphasic behavior suggests that below ~75 mM H_2O_2 a new, spectrally distinct species is present.

100% O_2 yielded no changes in absorbance after 2 h. Addition of five equivalents of H_2O_2 generated a brown solution (Figure 5). Exposure to intense visible light changed the brown solution to a pink solution (Figure 5).[5] No such spectral changes were observed upon addition of H_2O_2 to a designed mononuclear Co^{II} center in MBP (*33*).

MBP.Hc.E.I329F. An additional mutation, I329F, was constructed in MBP.Hc.E with the intent of altering the equilibrium between the open and closed states, to favor the latter (*33*). Titrations with $CuSO_4$ indicated that a Cu^{II}_2 complex is formed in this mutant, with a dissociation constant similar to MBP.Hc.E. Titration with H_2O_2 yielded a biphasic binding isotherm with different spectral species observed at low and high H_2O_2 concentrations, respectively. At low concentrations, a shoulder at 500 nm is observed, that disappears at high H_2O_2 concentrations (Figure 6). This biphasic behavior suggests the formation of two spectroscopically distinct species.

DISCUSSION

The *Dezymer* program was used to predict a small family of designs with His_6 primary coordination spheres to convert the wild-type maltose-binding site in MBP into an oxygen-binding site. The use of a family of designs allows multiple, independent starting points to be explored, recognizing that the predictions cannot be expected to be sufficiently accurate to guarantee success at this point in time. Out of these five starting points, we selected one family member, MBP.Hc.E, for more detailed characterization based on protein stability, Cu^{II} binding, and interactions with small ligands. Designs MBP.Hc.A−D were rejected primarily based on decreased protein stability and solubility. At this stage, it is not readily apparent why MBP.Hc.E is better behaved than the other designs.

As intended, MBP.Hc.E binds two equivalents of Cu^{II}. The resulting metalloprotein (Cu_2·MBP.Hc.E) binds small ligands such as N_3, H_2O_2, and O_2. Cu^{II}_2·MBP.Hc.E is not magnetically coupled, unless H_2O_2 is added, indicating that there is no significant electronic communication between the two Cu^{II} atoms in the absence of ligand, but that a bridged binuclear center does form upon addition of H_2O_2 (Cu^{II}_2·MBP.Hc.E·H_2O_2). One interpretation is that in the absence of H_2O_2 the two Cu^{II} are separated by more than 5 Å in Cu^{II}_2·MBP.Hc.E. This may be a consequence of the hinge-bending motions present in MBP. Cu^{II} binding by itself may not be sufficient to form the closed state, but the additional stabilization provided by a bridging ligand could be sufficient to shift the equilibrium toward a closed state. Examination of the structure of the design model suggests that the Cu−Cu distances can range from ~8 to 3.5 Å upon transition from the open to closed states, respectively (Figure 1D,E). In hemocyanin, this distance varies only from 2.5 to 4.5 Å (*35*). In model complexes, these distances can be substantially larger even than in MBP.Hc.E and is one of the critical determinants for the reactivity of these copper centers. The possibility of forming intermediate Cu−Cu distances may therefore play an important role in determining the properties of the Cu_2 center in MBP.Hc.E.

To examine the reactivity of Cu_2·MBP.Hc.E, we characterized two isoelectronic reactions: binding of H_2O_2 to Cu^{II}_2 and binding of O_2 to Cu^{I}_2. In both cases, a broad absorbance develops at 310 nm, and a species that retains these spectroscopic properties was isolated by gel filtration. The O_2-derived species has a less intense absorbance at 310 nm than the H_2O_2-derived species and is somewhat susceptible to loss of the metal center upon gel filtration. The dissocation constant of the H_2O_2 complex is 15 mM. The approximate concentration of dissolved O_2 is at most 1.2 mM at 25 °C (*36*). Therefore, in both methods of preparation the same species could be formed, with the O_2-derived species corresponding to concentrations well below saturation; alternatively, they represent chemically distinct species.

Extensive studies of binuclear copper oxygen model chemistry have produced numerous UV−visible spectroscopic fingerprints of binuclear copper oxygen coordination complexes (*10*, *20*, *21*). The UV−visible spectrum of oxy-Hc and a $[Cu^{II}_2(\mu-\eta^2:\eta^2\text{-}O_2)]^{2+}$ core in a synthetic model is distinguished by two broad transitions: at 350 nm ($\epsilon \sim 20\,000\ M^{-1}\ cm^{-1}$) and at 500−550 nm ($\epsilon \sim 1000\ M^{-1}\ cm^{-1}$) (*10*). The spectra of neither Cu^{I}_2·MBP.Hc.E·O_2 nor the Cu^{II}_2·MBP.Hc.E·H_2O_2 correspond to this spectrum. The less intense absorbance at 310 nm ($\epsilon_{310} \sim 3000\ M^{-1}\ cm^{-1}$) of Cu^{I}_2·MBP.Hc.E·O_2 could be consistent with a $[Cu^{II}_2(\mu\text{-}OH)_2]^{2+}$ core. The intensity of Cu^{II}_2·MBP.Hc.E·H_2O_2 ($\epsilon_{310} \sim 20\,000\ M^{-1}\ cm^{-1}$) matches the spectra of no reported copper oxygen complexes. However, the spectrum of Cu^{II}_2·MBP.Hc.E·H_2O_2 is similar to a diamagnetic complex with a $[Ni^{II}_2(\mu^{1,2}-O_2)_2]^{2+}$ core (*37*). The synthetic routes to this binuclear nickel complex (*37*), and an analogous cobalt complex (*38*−*40*), are quite similar to the peroxygenation reactions reported here. These model complexes have a more

[5] The observed photosensitivity of the Co^{II} H_2O_2 derivative unfortunately precludes characterization of visible-range CD or resonance Raman spectroscopies.

extended core structure than observed in type III centers, with a Cu−Cu distance of 6 Å, and have two equivalents of superoxide bridging the two metals, in a chair conformation. Therefore, it is likely that the Cu_2·MBP.Hc.E species do not adapt a structure that is similar to a oxy-Hc core.

Binuclear cobalt-substituted proteins (*41*−*43*) and model complexes (*38*−*40*, *44*−*46*) can mimic many of the important aspects of the binuclear Cu^{II}_2 centers. No spectral changes were observed upon addition of O_2 to Co^{II}_2·MBP.Hc.E, whereas addition of H_2O_2 forms a spectroscopically active complex (Co^{II}_2·MBP.Hc.E·H_2O_2). This is in direct contrast with Co^{II}_2-substituted hemocyanin, which forms a complex with O_2 but not with H_2O_2 (*41*−*43*), suggesting that the redox potentials of Co^{II}_2-hemocyanin and Co^{II}_2·MBP.Hc.E are substantially different. The spectrum of the Co^{II}_2·MBP.Hc.E·H_2O_2 brown species is similar to a model complex that has either a $[Co^{II}_2(\mu-\eta^2:\eta^2\text{-}O_2)]^{2+}$ or $[Co^{III}_2(\mu-O)_2]^{2+}$ core (350 nm, 8900 M^{-1} cm^{-1}; 493 nm, 2900 M^{-1} cm^{-1}) (*38*, *39*, *45*). The Co^{II}_2·MBP.Hc.E·H_2O_2 brown species is photosensitive, and upon prolonged illumination completely converts to a pink species that is spectroscopically similar to a model complex (*46*) with a $[Co^{II}_2(\mu\text{-}OH)_2]^{2+}$ core. These observations are consistent with the Co^{II}_2·MBP.Hc.E·H_2O_2 brown species containing a binuclear Co^{III} complex, that can be photoreduced to a $[Co^{II}_2(\mu\text{-}OH)_2]^{2+}$ core, the Co^{II}_2·MBP.Hc.E·H_2O_2 pink species, by the addition of two reduction equivalents (source not identified).[6] Such photoprocesses are well established for distorted five- or six-coordinate Co^{III} complexes (*47*, *48*). Taken together, these data are consistent with formation of metal−oxygen cores that are structurally similar to the oxy-hemocyanin core.

Comparison of the observed electronic absorbance spectra of the MBP.Hc.E Co_2 and Cu_2 complexes with those obtained for synthetic models and proteins of defined structure has allowed an initial structural assignment of the species observed in this designed protein suggesting that Cu_2·MBP.Hc.E does not form complexes with O_2 or H_2O_2 corresponding to the core structure of oxy-Hc, whereas the Co_2·MBP.Hc.E metalloprotein does appear to be able to do so. This suggests that a structure approximating the desired state can form in the Co_2 complex, but that in the case of the Cu_2 complexes, competing states are energetically more favorable, and form instead. One interpretation is that the hinge bending motions in MBP allow the core to adopt more elongated Cu−Cu distances than observed in the core structure of oxy-Hc. Stabilization of the closed state (or destabilization of the open state) is therefore predicted to alter the relative energies of these competing states, favoring states with shorter Cu−Cu distances.

It has been shown that mutations in the hinge, distal to the ligand-binding site, affect the equilibrium between the open and closed states (*33*). We therefore constructed I329F in MBP.Hc.E (MBP.Hc.E1), a mutation that is known to favor formation of the closed state. The Cu^{II}_2 sample of MBP.Hc.E1 shows a response to addition of H_2O_2 as compared to Cu^{II}_2·MBP.Hc.E (Figure 5). The apparent H_2O_2 affinity of Cu^{II}_2·MBP.Hc.E1 (observing changes at 310 nm) decreased from 15 to 40 mM. An additional absorbance[33] was observed at 500 nm ($\epsilon \sim 700$ M^{-1} cm^{-1}) at lower H_2O_2 concentrations. These results clearly demonstrate that a new, spectroscopically distinct species forms as the conformational equilibrium shifts toward the closed form. Of the binuclear copper−oxygen species reported here, this new species is the most spectroscopically similar to oxy-Hc. This strongly suggests that the strategy of shifting the equilibrium toward the closed form successfully alters the distribution of competing states, and stabilizes formation of a species approximating oxy-Hc. However, the I329F mutation is not sufficient to fully populate the closed conformation.

CONCLUSIONS

We have constructed a 10-fold mutant of MBP in which we successfully introduced a nascent binuclear copper oxygenase active site in place of the maltose-binding site, using computational methods to design the mutations. The new active site introduced into this novel protein, MBP.Hc.E, is intended to mimic properties of type III binuclear copper centers found in naturally evolved proteins such as hemocyanin. We have shown that MBP.Hc.E can form Cu^{II}_2 and Co^{II}_2 complexes that interact with H_2O_2 and O_2. The Co^{II}_2 protein reacts with H_2O_2 to form a complex that is spectroscopically similar to a synthetic model that structurally mimics the oxyhemocyanin core, whereas the Cu^{II}_2 protein reacted with O_2 or H_2O_2 does not. We postulate that the equilibrium between the open and closed conformations of MBP allows species with variable Cu−Cu distances to form, and that such species can bind ligands in geometries that are not observed in natural type III centers. Introduction of one additional mutation in the hinge, I329F, known to favor formation of the closed state, results in a binuclear copper center that when reacted with low concentrations of H_2O_2 mimics the spectroscopic signature of oxy-hemocyanin.

The existence of competing states and manipulation of their relative energies is emerging as a general theme in (metallo) protein design (*1*−*3*). There are two general routes available for the manipulation of the energy levels in the manifold of possible states: competing state destabilization or target state optimization (*5*, *6*, *8*). In the case of the Cu_2-MBP.Hc.E, the hinge bending motions present in MBP allow the core to adopt more elongated Cu−Cu distances than observed in the core structure of oxy-Hc, and stabilization of the closed state (or destabilization of the open state) alters the relative energies of such states, favoring states with shorter Cu−Cu distances. In hemocyanin, tyrosinase and catechol oxidase, the type III centers are located within the hydrophobic core of a four-helix bundle. This is a rigid environment, preventing the Cu−Cu distance from exceeding ~5 Å. Similarly, the designed binuclear iron centers are located in a rigid four-helix bundle (*49*). Interestingly, in this case it was necessary to decrease the rigidity of the environment to obtain enhanced ferrooxidase activity (*18*). The binuclear center in peptidylglycine α-hydroxy monooxygenase is located within an intersubunit interface, but is also in a rigid environment (*50*, *51*). In synthetic models, linker flexibility of dinucleating ligands has precluded the formation of $Cu^{II}_2(\mu-\eta^2:\eta^2\text{-}O_2^{2-})$ or $Cu^{III}_2(\mu-O)_2$ complexes at room temperature (*20*) until recently, when the use of more rigid linkers (*52*), dendrimer-substituted linkers (*53*), or CF_3-substituted ligands (*54*) was explored.

[6] A similar, reduced product appears to be formed upon addition of dithionite (data not shown).

Scheme 1: Proposed Mechanism for O_2- and H_2O_2-mediated Oxidations of Cu_2·MBP.Hc.E[a]

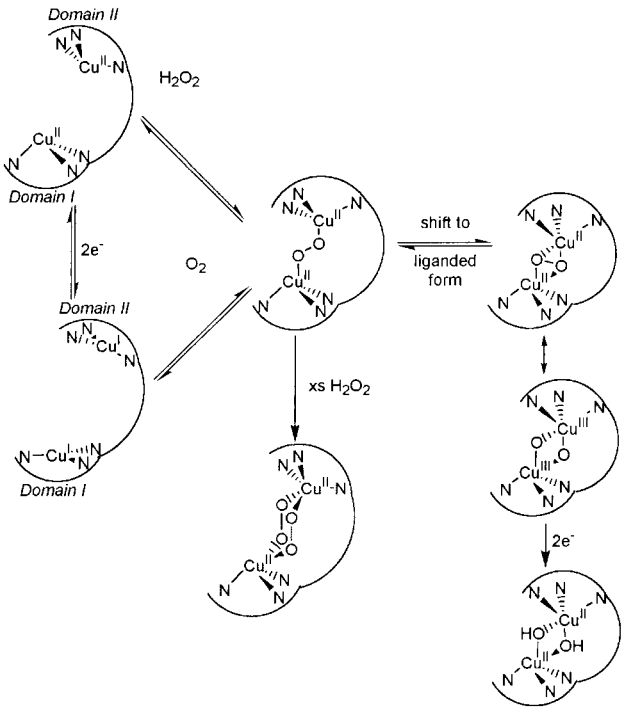

[a] See text.

We propose that the different species identified in Cu_2·MBP.Hc, and analogous Co_2·MBP.Hc species, are related according to Scheme 1. Upon the addition of H_2O_2 to Cu^{II}_2·MBP.Hc.E, or O_2 to Cu^{I}_2·MBP.Hc.E, in the open state (long Cu−Cu distances) a species (**3)** is formed that bridges the two copper centers in an extended conformation, which might be similar to the $[Cu^{II}_2(\mu^{1,2}-O_2)]^{2+}$ cores (*55*) recently implicated in the formation of oxy-hemocyanin (*35*). Addition of excess H_2O_2 in the open state is likely to lead to the formation of an additional species (**4**, corresponding to Cu^{II}_2·MBP.Hc.E·H_2O_2**)** that is spectroscopically distinct from known copper oxygen complexes seen in synthetic models or proteins. Since the protein is in equilibrium between the open and closed forms, formation of the closed form converts species **4** into species **5**, corresponding to Cu^{II}_2·MBP.Hc.E1·H_2O_2, observed at low H_2O_2 concentrations that has a shorter Cu−Cu distance. This shortening of the Cu−Cu distances is accompanied by an alteration of oxygen coordination geometry (from $\mu^{1,2}$ to $\mu-\eta^2:\eta^2$). Species **5** corresponds to the structure of oxy-Hc. The structural rearrangement from **4** to **5** is analogous to the transition from the T to R state recently proposed for oxy-Hc (*35*). It has been established that **5** can isomerize to **6**, which is postulated to be the reactive intermediate in the oxidation chemistries of tyrosinase and several synthetic models (*21*). The brown Co^{II}_2·MBP.Hc.E·H_2O_2 species is likely to be a structural analogue of **6** (*21*, *38*). Photoreduction of brown Co^{II}_2·MBP.Hc.E·H_2O_2 forms a pink species that is likely to correspond to **7**, and is structurally analogous to met-hemocyanin. The spectroscopic signature of Cu^{I}_2·MBP.Hc.E·O_2 is consistent either with **4** (subsaturated), or **7**. In the latter case, this implies that we are observing oxygen activation, and that MBP.Hc.E is a nascent oxidase, rather than the precursor to a reversible oxygen carrier protein.

ACKNOWLEDGMENT

We thank Drs. T. G. Spiro, C. M. Coyle, and Q. Wu for assistance with resonance Raman measurements.

REFERENCES

1. DeGrado, W. F., Summa, C. M., Pavone, V., Nastri, F., and Lombardi, A. (1999) *Annu. Rev. Biochem. 68*, 779−819.
2. Hellinga, H. W. (1996) in *Protein Engineering: Principles and Practice* (Cleland, J. L., and Craik, C. S., Eds.) pp 369−398, Wiley-Liss.
3. Gibney, B. R., and Dutton, P. L. (2001) *Adv. Inorg. Chem. 51*, 409−455.
4. Benson, D. E., Wisz, M. S., Liu, W., and Hellinga, H. W. (1998) *Biochemistry 37*, 7070−7076.
5. Hecht, M. H., Richardson, J. S., Richardson, D. C., and Ogden, R. C. (1990) *Science 249*, 884−891.
6. Hellinga, H. W. (1998) *Nat. Struct. Biol. 5*, 525−527.
7. Benson, D. E., Wisz, M. S., and Hellinga, H. W. (2000) *Proc. Natl. Acad. Sci. U.S.A. 97*, 6292−6297.
8. Hellinga, H. W. (1998) *J. Am. Chem. Soc. 120*, 10055−10066.
9. Wisz, M. S., Garrett, C. Z., and Hellinga, H. W. (1998) *Biochemistry 37*, 8269−8277.
10. Solomon, E. I., Sundaram, U. M., and Machonkin, T. E. (1996) *Chem. Rev. 96*, 2563−2605.
11. Tam, R., and Saier, M. H. (1993) *Microbiol. Rev. 57*, 320−346.
12. Quiocho, F. A., Spurlino, J. C., and Rodseth, L. E. (1997) *Structure 5*, 997−1015.
13. Gerstein, M., Lesk, A. M., and Chothia, C. (1994) *Biochemistry 33*, 6739−6749.
14. Valentine, J., Wertz, D., Lyons, T., Liou, L., Goto, J., and Gralla, E. (1998) *Curr. Opin. Chem. Biol. 2*, 253−262.
15. Arnold, F. (2001) *Nature 409*, 252−257.
16. Benson, D. E., Wisz, M. S., and Hellinga, H. W. (1998) *Curr. Opin. Biotechnol. 9*, 370−376.
17. Moffet, D. A., Certain, L. K., Smith, A. J., Kessel, A. J., Beckwith, K. A., and Hecht, M. H. (2000) *J. Am. Chem. Soc. 122*, 7612−7613.
18. Pasternak, A., Kaplan, J., Lear, J. D., and DeGrado, W. F. (2001) *Protein Sci. 10*, 958−969.
19. Lange, S. J., and Que, L. (1998) *Curr. Opin. Chem. Biol. 2*, 159−172.
20. Karlin, K. D., Tolman, W. B., Kanderli, S., and Zuberbuhler, A. D. (1997) *J. Mol. Catal. A: Chem. 117*, 215−222.
21. Blackman, A. G., and Tolam, W. B. (2000) *Struct. Bond. 97*, 179−211.
22. Glusker, J. P. (1991) *Adv. Prot. Chem. 42*, 1−76.
23. Holmquist, B. (1988) *Methods Enzymol. 158*, 6−13.
24. Hellinga, H. W., and Richards, F. M. (1991) *J. Mol. Biol. 222*, 763−785.
25. Sambrook, J., Fritsch, E. F., and Maniatis, T. (1989) *Molecular Cloning: A Laboratory Manual*, Vol. 3rd, 2nd ed., Cold Spring Harbor Press, Plainview, NY.
26. Sloan, D. J., and Hellinga, H. W. (1998) *Protein Eng. 11*, 819−823.
27. Gill, S. C., and von Hippel, P. H. (1989) *Anal. Biochem. 182*, 319−326.
28. Bradford, M. M. (1976) *Anal. Biochem. 72*, 248−254.
29. Creighton, T. E. (1993) *Proteins: Structure and Molecular Properties*, 2nd ed., W. H. Freeman and Co., New York.
30. Evans, P. J., and Halliwell, B. (1994) *Methods Enzymol. 233*, 82−92.
31. Hazes, B., Magnus, K. A., Bonaventura, C., Bonaventura, J., Dauter, Z., Kalk, K. H., and Hol, W. G. J. (1993) *Protein Sci. 2*, 597−609.
32. Kitajima, N., and Moro-Oka, Y. (1994) *Chem. Rev. 94*, 737−757.
33. Marvin, J. S., and Hellinga, H. W. (2001) *Nat. Struct. Biol., 8*, 795−798.
34. Azulet, G., Bubacco, L., Casella, L., Rocco, G. P., Salvato, B., and Beltramini, M. (1997) *Eur. J. Biochem. 247*, 688−694.

35. Metz, M., and Solomon, E. I. (2001) *J. Am. Chem. Soc. 123*, 4938−4950.
36. Battino, R. (1981) in *IUPAC Solubility Data Series* (Battino, R., Ed.), Pergammon Press, Oxford, England.
37. Shiren, K., Ogo, S., Fujinami, S., Hayashi, H., Suzuki, M., Uehara, A., Watanabe, Y., and Moro-oka, Y. (2000) *J. Am. Chem. Soc. 122*, 254−262.
38. Hikichi, S., Akita, M., and Moro-Oka, Y. (2000) *Coord. Chem. Rev. 198*, 61−87.
39. Hikichi, S., Yoshizawa, M., Sasakura, Y., Akita, M., and Moro-Oka, Y. (1998) *J. Am. Chem. Soc. 120*, 10567−10568.
40. Reinaud, O. M., Yap, G. P. A., Rheingold, A. L., and Theopold, K. H. (1995) *Angew. Chem., Int. Ed. 34*, 2051−2052.
41. Larrabee, J. A., Baumann, T. F., Chisdes, S. J., and Lyons, T. J. (1992) *Inorg. Chem. 31*, 3630−3635.
42. Dutton, T. J., and Larrabee, J. A. (1990) *Inorg. Chem. 29*, 2272−2278.
43. Huber, M., Bubacco, L., Beltramini, M., Salvato, B., Elias, H., Peisach, J., Larsen, E., Harnung, S. E., and Haase, W. (1996) *Inorg. Chem. 35*, 7482−7492.
44. He, C., and Lippard, S. J. (1998) *J. Am. Chem. Soc. 120*, 105−113.
45. Hikichi, S., Komatsuzaki, H., Kitajima, N., Akita, M., Mukai, M., Kitagawa, T., and Moro-Oka, Y. (1997) *Inorg. Chem. 36*, 266−270.
46. Kitajima, N., Hikichi, S., Tanaka, M., and Moro-oka, Y. (1993) *J. Am. Chem. Soc. 115*, 5496−5508.
47. MacArther, R., Sucheta, A., Chong, F. F. S., and Einarsdottir, O. (1995) *Proc. Natl. Acad. Sci. U.S.A. 92*, 8105−8109.
48. Lever, A. B. P., and Gray, H. B. (1978) *Acc. Chem. Res. 11*, 348−355.
49. Lombardi, A., Summa, C. M., Geremia, S., Randaccio, L., Pavone, V., and DeGrado, W. F. (2000) *Proc. Natl. Acad. Sci. U.S.A. 97*, 6298−6305.
50. Prigge, S. T., Kolhekar, A. S., Eipper, B. A., Mains, R. E., and Amzel, L. M. (1997) *Science 278*, 1300−1305.
51. Prigge, S. T., Kolhekar, A. S., Eipper, B. A., Mains, R. E., and Amzel, L. M. (1999) *Nat. Struct. Biol. 6*, 976−983.
52. Kodera, M., Katayama, K., Tachi, Y., Kano, K., Hirota, S., Fujinami, S., and Suzuki, M. (1999) *J. Am. Chem. Soc. 121*, 11006−11007.
53. Enomoto, M., and Aida, T. (1999) *J. Am. Chem. Soc. 121*, 874−875.
54. Hu, Z., Williams, R. D., Tran, D., Spiro, T. G., and Gorun, S. M. (2000) *J. Am. Chem. Soc. 122*, 3556−3557.
55. Paul, P. P., Tyeklar, Z., Jacobson, R. R., and Karlin, K. D. (1991) *J. Am. Chem. Soc. 113*, 5322−5332.
56. Spurlino, J. C., Lu, G. Y., and Quiocho, F. A. (1991) *J. Biol. Chem. 266*, 5202−19.
57. Kraulis, P. (1991) *J. Appl. Crystallogr. 24*, 946−950.

BI011359I